Available online at www.sciencedirect.com
ScienceDirect
Journal of Organometallic Chemistry 692 (2007) 142–147
Journal of Organometallic Chemistry
www.elsevier.com/locate/jorganchem

Design of artificial metalloenzymes using non-covalent insertion of a metal complex into a protein scaffold

Takafumi Ueno [a,*], Tomomi Koshiyama [b], Satoshi Abe [b], Norihiko Yokoi [b], Masataka Ohashi [c], Hiroshi Nakajima [b], Yoshihito Watanabe [b,*]

[a] *Research Center for Materials Science, Nagoya University, Nagoya 464-8602, Japan*
[b] *Department of Chemistry, Graduate School of Science, Nagoya University, Nagoya 464-8602, Japan*
[c] *Department of Structural Molecular Science, The Graduate University for Advanced Studies, Okazaki 444-8585, Japan*

Received 27 February 2006; received in revised form 29 May 2006; accepted 2 June 2006
Available online 30 August 2006

Abstract

Construction of artificial metalloenzymes is one of the most attractive targets in the field of inorganic and catalytic chemistry, since they show remarkable chemoselectivity and reactivity in aqueous media. For the purpose, covalent modification of protein and cofactors have usually been utilized to attach a metal complex(es) to a protein scaffold. This article focuses on non-covalent insertion of metal complexes into protein environments. The discussion includes the screening of stable metal complex/protein composites, crystal structures, molecular design for regulating enantioselectivity of the target catalytic reactions. Our recent results show that the non-covalent conjugation will provide us a new way in semi-synthesis of artificial metalloenzymes.

Keywords: Myoglobin; Schiff base; Oxygenation; Sulfoxidation; Metalloenzyme; Heme

1. Introduction

Recently, construction of bio-conjugated metal catalysts has become an important topic in bioinorganic chemistry [1–4]. They have great possibilities for their high catalytic reactivity and selectivity in aqueous media. Traditional preparation of metal complex/protein composites has been divided in three distinct methods: (i) covalent anchoring to amino acid residues [5–7], (ii) conjugation of metal ligands to native substrates [8–10], and (iii) modification of native metal cofactors [11,12]. Although the last two methods are very convenient to introduce many functions into proteins, there are limitations in type of proteins to be used for this purpose and in synthesis of modified substrates and cofactors. If synthetic metal compounds can be introduced into protein cages as simple as the heme prosthetic group that is non-covalently bound in the cavity of heme proteins, the bio-conjugation of metal complexes will be applicable to many proteins and metal complexes (Scheme 1). Thus, we have developed a new method for the preparation of metal complexes placed in protein cavities by non-covalent fixation [13]. In this paper, we describe the screening of non-covalent insertion of Schiff base complexes into apo-myoglobin cavity and the molecular design of metal complex/protein composites based on their crystal structures to improve the catalytic reactivity [14,15].

2. Non-covalent insertion of Schiff base complexes into apo-Mb

As the target protein and metal complexes to be conjugated together, we have employed myoglobin (Mb) and Schiff base complexes, respectively. Mb, a hemeprotein responsible for O_2 storage in muscle, has a cavity of ca. 10 Å diameter to accommodate heme (Fig. 1a) [16]. The affinity of heme for apo-myoglobin (apo-Mb) results from:

* Corresponding author. Tel./fax: +81 52 789 2953.
E-mail address: taka@mbox.chem.nagoya-u.ac.jp (T. Ueno).

0022-328X/$ - see front matter © 2006 Elsevier B.V. All rights reserved.
doi:10.1016/j.jorganchem.2006.08.043

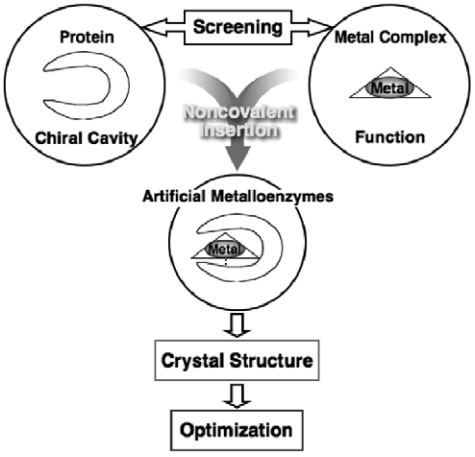

Scheme 1. Design concept for the optimization of catalytic reactivity of artificial metalloenzymes constructed with non-covalent insertion.

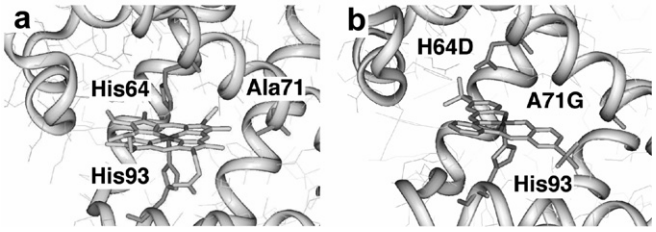

Fig. 1. Active site structures of wild-type Mb taken from PDB ID: 2MBW (a) and **Cr · 7 · apo-A71GMb** calculated by INSIGHTII/DISCOVER 3 program (ESFF force field) (b). The interacted sidechains with heme and **Cr · 7** are shown with stick models.

(i) hydrogen bond and hydrophobic interactions between the protein and heme; and (ii) the coordination of the proximal His93 ligand to the heme iron [17]. Schiff base complexes containing Mn(III) and Cr(III) have been reported as oxidation catalysts in organic solvents [18–21]. Advantage of Schiff base complexes for the heme substitution is that their molecular size and coordination geometry are almost identical to heme and it is easy to modify the ligand size and hydrophobicity. Typical reconstitution procedure of a Schiff base complex with apo-Mb is shown in Scheme 2b. Heme is removed from Mb by a HCl/2-butanone method as reported previously [22], and then the composite is obtained by adding a methanol solution of a Schiff base complex into the apo-Mb solution [15].

We have designed an apo-Mb mutant suitable both for the reconstitution with Schiff base complexes and for the catalytic reactions using Insight II/Discover 3. If we assume that **Cr · 7** binds to His93 as observed for heme, the alanyl sidechain at the position 71 in Mb is expected to locate very much close to the 4 and 5 positions of **Cr · 7** (Fig. 1b). Thus, Ala71 was replaced to Gly in order to improve the binding affinity of **Cr · 7** in the active site. In addition, the replacement of His64 to Asp (H64D) is expected to increase access of substrates and oxidants to a vacant distal site above the Cr(III) center. Unfortunately, **Cr · 7 · apo-H64D/A71GMb** shows low reactivity and enantioselectivity in thioanisole sulfoxidation (Table 1) [13]. In order to improve the catalytic activity as well as enantioselectivity, we need to know the structure of M(Schiff base)apo-Mb composites (M = Cr, Mn, and Fe). Thus, we have attempted the screening of stable M(Schiff base)apo-Mb composites for the crystal structure studies.

3. Screening of Schiff base ligands having higher affinity for apo-Mb

For the determination of Cr(III) complexes having high affinity to apo-A71GMb, we have used electrospray

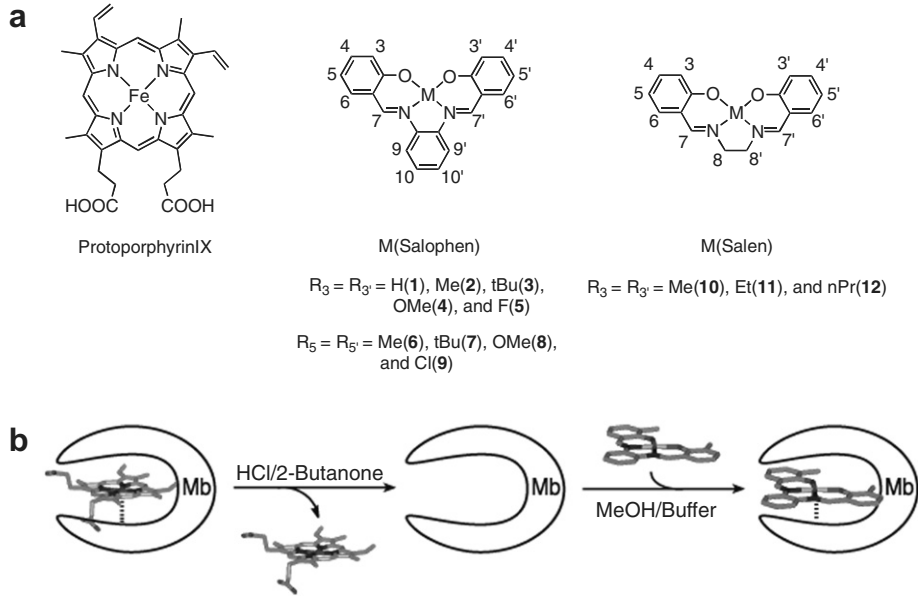

Scheme 2. Molecular structures of heme and Schiff base complexes (a) and typical preparation scheme of Schiff base complex/apo-Mb composites (b).

Table 1
Enantioselective thioanisole sulfoxidation[a]

Catalyst	Rate[b]	% ee
Cr · 1 · apo-H64D/A71GMb	83 ± 3	8 ± 0.5 (*S*)
Cr · 2 · apo-A71GMb	22 ± 3	5 ± 0.2 (*S*)
Cr · 2 · apo-H64D/A71GMb	130 ± 6	30 ± 1.1 (*S*)
Cr · 7 · apo-Mb	46	4.3 (*R*)
Cr · 7 · apo-H64DMb	27	0.3 (*S*)
Cr · 7 · apo-A71GMb	54	6 (*S*)
Cr · 7 · apo-H64D/A71GMb	78	13 (*S*)
Cr · 10 · apo-H64D/A71GMb	210 ± 76	33 ± 1.6 (*S*)
Cr · 11 · apo-H64D/A71GMb	48 ± 1	14 ± 0.2 (S)
Cr · 12 · apo-H64D/A71GMb	43 ± 4	12 ± 0.1 (S)
Mn · 10 · apo-A71GMb	1295 ± 119	17 ± 0.6 (*R*)
Mn · 11 · apo-A71GMb	803 ± 5	23 ± 0.2 (*R*)
Mn · 12 · apo-A71GMb	2724 ± 69	27 ± 0.1 (*R*)
Mn · 2 · apo-H64D/A71GMb	158 ± 8	23 ± 0.5 (*S*)
Mn · 10 · apo-H64D/A71GMb	464 ± 62	32 ± 0.1 (*S*)
Mn · 11 · apo-H64D/A71GMb	135 ± 5	5 ± 0.7 (*S*)
Mn · 12 · apo-H64D/A71GMb	180 ± 7	13 ± 0.5 (*R*)
Mn · 10 in buffer	62 ± 3	0
Mn · 11 in buffer	39 ± 6	0
Mn · 12 in buffer	87 ± 6	0

[a] Sulfoxidation was carried out in sodium acetate buffer (50 mM, pH 5.0) at 35 °C in the presence of a Mb composite (10 μM), thioanisole (1 mM), and H_2O_2 (1 mM) [13,14].
[b] The unit of the rate is 10^{-3} turnover min^{-1}.

ionization-time of flight mass spectrometry (ESI-TOF MS). The mass spectrum of a mixture of Cr(Schiff base) complex and apo-A71GMb in 5 mM ammonium acetate buffer (pH 6.4) gave two peaks corresponding to Cr(Schiff base) · apo-A71GMb and apo-A71GMb (Fig. 2a). In order to estimate the affinity of Cr(Schiff base) with the apo-Mb mutant, we have compared stability of the composites with [Cr(Schiff-base) · apo-A71GMb]/([Cr(Schiff-base) · apo-A71GMb] + [apo-A71GMb]) ratio of the ESI-TOF MS peak intensity as shown in Fig. 2b. **Cr · 2** and **Cr · 3** have the largest values among the screened ligands though the values of the other 3-,3′-substituted salophens are almost comparable with those of 5- and 5′-substituted salophens. The screening results suggest that alkyl groups as methyl or *t*-Bu at the 3 and 3′ positions of salophen have specific interactions with the neighboring amino acid residues in Mb heme cavity. Thus, we have attempted to determine the crystal structures of **M · 2 · apo-A71GMbs** to find the interactions to hold the composites stable in the inside of apo-Mb mutants.

4. Crystal structures of M(Schiff base)apo-Mb composites

Crystal structures of **Cr · 2 · apo-A71GMb** and **Mn · 2 · apo-A71GMb** were determined at 1.45 Å resolution. As shown in Fig. 3a, they are located in the heme cavity with the same coordination geometry. For example, **Cr · 2** is fixed in the cavity by ligating the chromium atom to His93 with a Cr–Nε distance of 2.13 Å. The distance is comparable to 2.07 and 2.17 Å of $[Cr^{III}(salen)(3\text{-}MeIm)_2]^+$ [23]. A water molecule binds tightly to the Cr atom at 2.00 Å, similar to those of $[Cr(salen)(H_2O)_2]^+$ (2.09 and 1.92 Å) [24]. On the other hand, **Mn · 2** exhibits longer bond distances with His93 and H_2O compared to those of **Cr · 2 · apo-A71GMb** (Fig. 3b). The bond distances are similar to those of $[Mn^{III}(7,7'\text{-}Ph_2\text{-}salen)(Py)_2]^+$ and $[Mn^{III}(3,3'\text{-}OMe_2\text{-}salen)(H_2O)_2]^+$ [21,25].

The orientation of **Mn · 2** in the cavity of apo-A71GMb is constrained by several specific interactions as shown in Fig. 3a. Phe43, Leu89 and Ile99 are located within the distances of π–π and CH–π interactions to **Mn · 2** [26]. Further, the C5 atom is close to the Cα atom of Ala71Gly

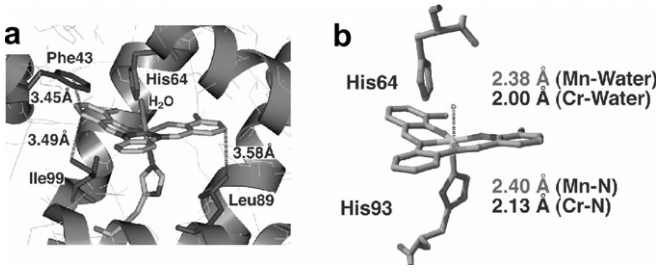

Fig. 3. Active site structure of **Mn · 2 · apo-A71GMb**: closed interactions with sidechains (a) and comparison in selected bond length with **Cr · 2 · apo-A71GMb** (b).

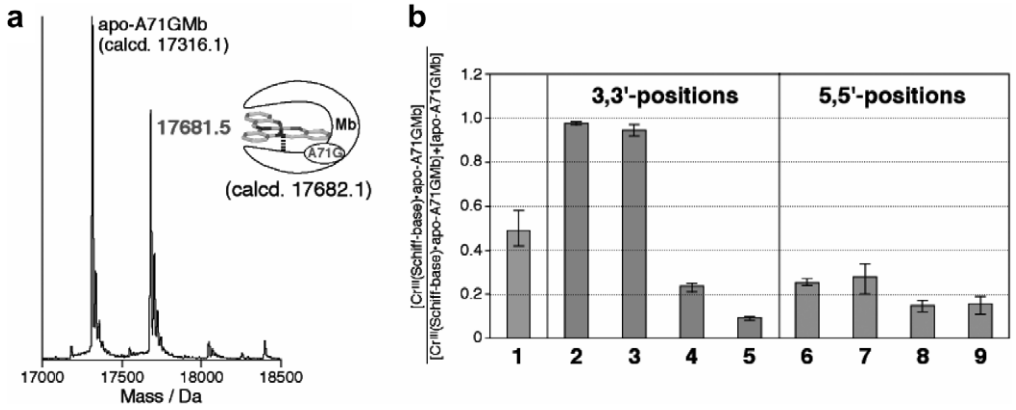

Fig. 2. ESI-TOF MS spectrum of **Cr · 2 · apo-A71GMb** (a) and screening results of Cr(Schiff base) complexes with apo-A71G Mb using ESI-TOF MS (b).

with a distance of 4.08 Å. On the other hand, a remarkable difference is observed for the electron density of a Schiff base complex in the active site of native apo-Mb, i.e., we are not able to determine the unique location of the metal complex even though the spectroscopic data of **Fe · 2 · apo-Mb** support the incorporation of **Fe · 2** in apo-Mb [15]. The steric repulsion of the C5 atom and Ala71 is predicted in our molecular modeling study [13] and this is the reason why we have prepared the Ala71Gly mutant. The crystal structure of **Cr · 2 · apo-A71GMb** shows that **2** just fills the cavity with two 3,3′-methyl groups as shown in Fig. 4a [14]. On the other hand, the calculated structure of **Cr · 7 · apo-A71GMb** suggests that a *t*-Bu group at the position of 5 is exposed to the solvent (Fig. 4b). Thus, the stability of **Cr · 7 · apo-A71GMb** is expected to be smaller than **Cr · 2 · apo-A71GMb**. In fact, the ESI-TOF MS peak ratio of **2** in Fig. 2b is larger than that of **7**. The comparison suggests that the crystal structures explain the stability estimated by the ESI-TOF MS screening.

Fig. 5a shows the superimposition of the active sites of **Mn · 2 · apo-A71GMb** and met-Mb. The Mn atom is located much deeper (1.41 Å) compared to the heme iron in the active site. The vinyl and methyl groups at the 2,3-position of heme have hydrophobic interactions with Ile107. It appears that they control the penetration depth of heme into the pocket [27]. Porphyrin and biliverdin ligands, which have no specific interactions with Ile107, are inserted deeper in the heme pocket than heme in met-Mb [28,29]. In the case of **Mn · 2 · apo-A71GMb**, the two methyl groups at the 3,3′-positions in **2** also show hydrophobic interaction with Ile107. They permit the Mn complex to be held deeper in the heme pocket. It is clear that the 3- and 3′-methyl groups and Ala71Gly mutation regulate the location and orientation of a Schiff base ligand in the heme cavity.

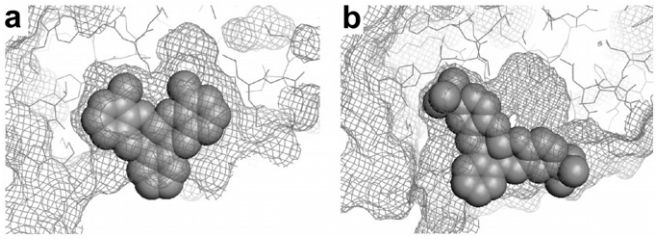

Fig. 4. Binding modes at the active sites of **Cr · 2 · apo-A71GMb** taken from PDB ID 1J3F (a) and **Cr · 7 · apo-A71GMb** calculated by INSIGHTII/DISCOVER 3.0 (b).

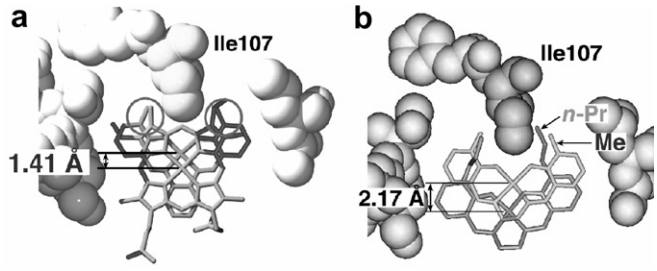

Fig. 5. The active site structure of **Mn · 2 · apo-A71GMb** superimposed on wild-type Mb (a) and calculated structure of **Mn · 10 · apo-H64D/A71GMb** superimposed on **Mn · 12 · apo-H64D/A71GMb** (b). The calculations were performed with INSIGHTII/DISCOVER 3 using the ESFF force field.

5. Crystal structure based molecular design of Schiff base complexes

On the basis of these crystal structures, we have designed Schiff base ligands to improve their catalytic reactivity in the heme cavity as shown in Fig. 5b. It is known that the accessibility of substrates is limited by the steric hindrance of heme and His64 [30]. The crystal structure of **Mn · 2 · apo-A71GMb** shows a narrow channel between His64 and the phenylenediamine unit of **2** (Fig. 3a). Thus, the unit was substituted by an ethylenediamine unit to enlarge the active site of **Mn · 2 · apo-A71GMb**. The position of the metal complex in the active site is an important factor to determine the selectivity of substrate oxidation. The position of **Mn · 2** in apo-A71GMb is regulated by several types of interaction, especially, the hydrophobic interaction between Ile107 and the 3 and 3′-methyl groups of **2**. Thus, the two methyl groups were substituted either by ethyl or by *n*-propyl groups to change the penetration depth of Mn(Schiff base) complexes in the protein. Energy minimization of the composites suggest that the Mn atoms are exposed to the outside of the cavity by 0.83 Å and 2.17 Å compared to that of **Mn · 10** (Fig. 5b) due to the Et and *n*-Pr substitutions, respectively. The enantioselective sulfoxidation catalyzed by these composites is discussed later.

6. Reactivity of Schiff base complexes in apo-Mb cavity

The H_2O_2-dependent sulfoxidation of thioanisole was examined at 35 °C (50 mM sodium acetate buffer, pH 5.0) and the results of the sulfoxidation are listed in Table 1. The oxidation rates by Cr and Mn Schiff base complexes are accelerated by insertion of them in apo-Mb. **Cr · 10 · apo-H64D/A71GMb** and **Cr · 7 · apo-H64D/A71GMb** exhibit 15- and 6-fold higher activities than that of **Cr · 7** in buffer, respectively [13]. Further, Mn(salen derivative)apo-A71GMbs show 21–31-fold increased rates than those of Mn(salen derivative) in the same buffer solution (Table 1). The Cr and Mn Schiff base complexes are known to catalyze the sulfoxidation of thioethers through the oxo transfer from Mn^{V}=O and Cr^{V}=O, respectively [31,32]. Kochi et al. have studied the catalytic oxidation by Cr(Schiff base) complexes in acetonitrile, and observed the enhancement of the catalytic reactivity by the addition of neutral donor ligand, such as pyridine and pyridine *N*-oxide [20,33]. The axial ligation is expected to weaken the Cr^{V}=O bond, which accounts for the increased reactivity of the 6-coordinate oxochromium(V) cation [20]. We have previously confirmed the formation of oxochromium(V) cation in **Cr · 7 · apo-H64D/A71GMb** [13]. The oxochromium(V) cation could be activated by the

axial ligation of His93 to the Cr atom in the hydrophobic cavity. Mn(Schiff base) complexes also require donor ligands such as imidazole to stabilize the highly reactive Mn^{V}=O (salen) species formed by the addition of H_2O_2 and to accelerate the rate of oxidation [34]. These results indicate that the imidazole ligation (His93) to the Cr and Mn atoms efficiently activates the M^{V}=O bond in the active site although a large excess of the donor ligands is required in the salen-catalyzed oxidation in organic solvents [20,21].

In addition, we have designed an enlarged cavity by the replacement of **2** with **10**, to increase the accessibility of substrates. The rate with **Mn · 10 · apo-H64D/A71GMb** is 3-fold higher than that with **Mn · 2 · apo-H64D/A71GMb**.

7. Regulation of the enantioselectivity in sulfoxidation

The crystal structure of **Mn · 2 · apo-A71GMb** shows hydrophobic interaction between the 3- and 3′-methyl groups and Ile107 (Fig. 5a). As discussed before, the replacement of the methyl groups with bulky ethyl and *n*-propyl groups is expected to change the position of the metal ion. Molecular modeling calculation of Mn(3,3′-X_2-salen)apo-H64D/A71GMbs (X = Me, Et, and *n*-Pr) indicates that the Mn atoms of **Mn · 11** and **Mn · 12** in the protein locate 0.83 and 2.17 Å outside from the position of **Mn · 10**, respectively (Fig. 5b). In addition, the calculation suggests that the position of thioanisole in the three composites is not changed since the replacement of two methyl groups with Et or *n*-Pr does not affect the interaction of the phenyl group in thioanisole with Phe43 and Leu32 (Fig. 6). These considerations indicate that the relative position of the sulfur atom and the oxo-metal center could be altered, resulting in the change of enantioselectivity in the sulfoxidation. In order to prove these ideas, the % ee values of the thioanisole oxidation catalyzed by a series of **Mn · 10 · apo-H64D/A71GMb**, **Mn · 11 · apo-H64D/A71GMb**, and **Mn · 12 · apo-H64D/A71GMb** were evaluated (Table 1). While **Mn · 10 · apo-H64D/A71GMb** showed 32% ee (*S*) selectivity, introduction of bulkier groups at the 3,3′-positions induces relative *R*-selectivity to end up 13% (*R*) for **12**. A series of Cr(3,3′-X_2-salen)apo-H64D/A71GMb and Mn(3,3′-X_2-salen)apo-H64D/A71GMb (X = Me, Et, and *n*-Pr) show the same trend in enantioselective sulfoxidation.

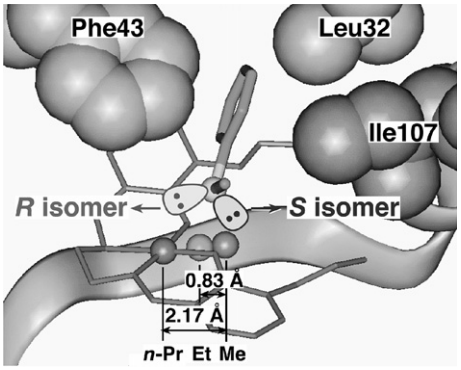

Fig. 6. Proposed mechanism of the enantioselective thioanisole sulfoxidation catalyzed by Mn(3,3′-X_2-salen) · apo-H64D/A71GMbs (X = Me, Et, and *n*-Pr).

8. Concluding remarks and future respects

The current goal for the construction of metal complex/protein composites is to create semi-synthetic metalloenzymes having high and controllable enantioselectivity in many catalytic reactions in aqueous media. In this account, we have described new method by non-covalent insertion of metal complexes instead of the typical covalent conjugations. Actually, the results support that the enantioselectivity and reactivity of catalytic reactions in protein cavities can be regulated without covalently anchoring of metal complexes. Furthermore, our method can be extended to various proteins and functions. For example, we have utilized protein–protein electron transfer systems and a nano-space consisted of a protein assembly for activation and concentration of metal complexes, respectively. We believe that the results will provide intriguing implication on application not only for catalysts, sensors, electronics devices, and so on.

Acknowledgements

This work was supported by 21st Century COE program of Nagoya University for T.K., S.A., and N.Y., and Grant-in-Aid for Scientific Research on Priority Areas (No. 16033226, "Reaction Control of Dynamic Complexes" and No. 16074208, "Chemistry of Coordination Space" for H.N. and Y.W., respectively) from Ministry of Education, Culture, Sports, Science and Technology, Japan.

References

[1] Y. Lu, S.M. Berry, T.D. Pfister, Chem. Rev. 101 (2001) 3047.
[2] Y. Lu, Curr. Opin. Chem. Biol. 9 (2005) 118.
[3] D. Qi, C.-M. Tann, D. Haring, M.D. Distefano, Chem. Rev. 101 (2001) 3081.
[4] C.M. Thomas, T.R. Ward, Chem. Soc. Rev. 34 (2005) 337.
[5] J.R. Carey, S.K. Ma, T.D. Pfister, D.K. Garner, H.K. Kim, J.A. Abramite, Z. Wang, Z. Guo, Y. Lu, J. Am. Chem. Soc. 126 (2004) 10812.
[6] R.R. Davies, M.D. Distefano, J. Am. Chem. Soc. 119 (1997) 11643.
[7] G.T. Hermanson, Bioconjugate Techniques, Academic Press, San Diego, 1996.
[8] C. Letondor, N. Humbert, T.R. Ward, Proc. Natl. Acad. Sci. USA 102 (2005) 4683.
[9] M. Skander, N. Humbert, J. Collot, J. Gradinaru, G. Klein, A. Loosli, J. Sauser, A. Zocchi, F. Gilardoni, T.R. Ward, J. Am. Chem. Soc. 126 (2004).
[10] M.E. Wilson, G.M. Whitesides, J. Am. Chem. Soc. 100 (1978) 306.
[11] I. Hamachi, S. Shinkai, Euro. J. Org. Chem. (1999) 539.
[12] T. Hayashi, Y. Hisaeda, Acc. Chem. Res. 35 (2002) 35.
[13] M. Ohashi, T. Koshiyama, T. Ueno, M. Yanase, H. Fujii, Y. Watanabe, Angew. Chem., Int. Ed. 42 (2003) 1005.

[14] T. Ueno, T. Koshiyama, M. Ohashi, K. Kondo, M. Kono, A. Suzuki, T. Yamane, Y. Watanabe, J. Am. Chem. Soc. 127 (2005) 6556.
[15] T. Ueno, M. Ohashi, M. Kono, K. Kondo, A. Suzuki, T. Yamane, Y. Watanabe, Inorg. Chem. 43 (2004) 2852.
[16] A. Messerschmidt, R. Huber, K. Wieghardt, T. PoulosHandbook of Metalloproteins, vol. 1, Wiley, 2001.
[17] C.L. Hunter, E. Lloyd, L.D. Eltis, S.P. Rafferty, H. Lee, M. Smith, A.G. Mauk, Biochemistry 36 (1997) 1010.
[18] E.N. JacobsenComprehensive Organometallic Chemistry II, vol. 12, Pergamon, New York, 1995.
[19] T. Katsuki, Coord. Chem. Rev. 140 (1995) 189.
[20] E.G. Samsel, K. Srinivasan, J.K. Kochi, J. Am. Chem. Soc. 107 (1985) 7606.
[21] K. Srinivasan, P. Michaud, J.K. Kochi, J. Am. Chem. Soc. 108 (1986) 2309.
[22] F. Ascoli, M. Fanelli, E. Antonini, Methods Enzymol. 76 (1981) 72.
[23] N. Matsumoto, K. Inoue, H. Okawa, S. Kida, Chem. Lett. (1989) 1251.
[24] P. Coggon, A.T. Mcphail, P.E. Mabbs, A. Richards, A.S. Thornley, J. Chem. Soc. (A) (1970) 3296.
[25] C.G. Zhang, G.H. Tian, Z.F. Ma, D.Y. Yan, Transition Met. Chem. 25 (2000) 270.
[26] M. Nishio, M. Hirota, Y. Umezawa, THE CH/π Interaction Evidence, Nature, and Consequences, Wiley-VCH, New York, 1998.
[27] T. Takano, J. Mol. Biol. 110 (1977) 537.
[28] S. Neya, N. Funasaki, T. Sato, N. Igarashi, N. Tanaka, J. Biol. Chem. 268 (1993) 8935.
[29] U.G. Wagner, N. Muller, W. Schmitzberger, H. Falk, C. Kratky, J. Mol. Biol. 247 (1995) 326.
[30] H.-J. Yang, T. Matsui, S.-i. Ozaki, S. Kato, T. Ueno, J.GeorgeN. Phillips, S. Fukuzumi, Y. Watanabe, Biochemistry 42 (2003) 10174.
[31] M. Palucki, P. Hanson, E.N. Jacobsen, Tetrahedron Lett. 33 (1992) 7111.
[32] N.S. Venkataramanan, S. Premsingh, S. Rajagopal, K. Pitchumani, J. Org. Chem. 68 (2003) 7460.
[33] K. Srinivasan, J.K. Kochi, Inorg. Chem. 24 (1985) 4671.
[34] A. Berkessel, M. Frauenkron, T. Schwenkreis, A. Steinmetz, G. Baum, D. Fenske, J. Mol. Cat. A: Chem. 113 (1996) 321.